Rate of neuronal turnover in the healthy adult murine myenteric ganglia varies with ganglia size

Anastazja M. Gorecki[1, 2], Alpana Singh[3], Chengxiu Zhang[3], Rohin Gurumurthy[3], Subhash Kulkarni[3#]

[1]Perron Institute for Neurological and Translational Science, Nedlands, Australia.

[2]School of Biological Sciences, University of Western Australia, Crawley, Australia.

[3]Center for Neurogastroenterology, Department of Medicine, Johns Hopkins University – School of Medicine, Baltimore, MD USA

[#]Address all correspondence to:

Subhash Kulkarni, Ph.D.

Assistant Professor

Department of Medicine

skulkar9@jh.edu

Abstract:

Major gastrointestinal and systemic functions are regulated by the Enteric Nervous System (ENS), whose cells are organized in interconnected clusters or ganglia to form plexuses in the gut wall. Previously, we showed that neuronal turnover, driven by overall equal rates of neurogenesis and neuronal loss, is an important homeostatic mechanism that maintains the larger myenteric plexus of the healthy adult ENS. While this process maintains neuronal numbers, whether it occurs at the same rate across the two sexes, in different regions and within ganglia that contain a diversity of neuronal numbers remains unknown. Here, by using antibodies against the DNA replication marker phospho-Histone H3 and against the pan-neuronal marker Hu to detect new-born neurons, we observe that while the proportions of new-born myenteric neurons are conserved irrespective of the region or sex in the healthy small intestine, they are inversely correlated with ganglia size. In contrast, by using antibodies against the apoptosis marker Cleaved Caspase 3 and Hu, we found that proportions of apoptotic neurons were directly correlated with ganglia size. Our observations on the unequal rate of neuronal turnover across ganglia, where smaller ganglia are more neurogenic and larger ganglia are more apoptotic, suggests that the myenteric ganglia are plastic in nature. These results provide further insight into the dynamic nature of the adult ENS.

Introduction:

The cells of the enteric nervous system (ENS) are located entirely within the gut wall and are routinely exposed to significant and continual mechanical stress and chemical insults from luminal contents[1-3]. Despite these ongoing and significant stressors, the question of how the adult ENS maintains itself has not been adequately addressed, especially given some prior studies reported that a significant proportion of enteric neurons undergo apoptosis at steady state[4-6].

In a previous report, we reported the presence of a neurogenic mechanism, which gives rise to a significant number of new neurons at steady state in the adult gut[7]. Using thymidine analogue studies and multiple lines of evidence to test for neuronal apoptosis, we demonstrated that the adult enteric neurogenic program replaces ~10% of apoptotic neurons every day, thus maintaining the structural and functional integrity of the adult ENS. In addition, our recent work also defined the normal structure of the adult murine ileal myenteric plexus, demonstrating that ganglia size, as defined by their neuronal numbers, is extremely heterogenous. We showed that myenteric ganglia contained between 3 to 150 neurons, but the relative distribution was heavily skewed towards smaller ganglia[8]. This remarkable heterogeneity in ganglia size begs the question whether the rate of neuronal turnover is constant in all myenteric ganglia, irrespective of their size. Another question that emerged from this study was whether the rate of neurogenesis was conserved in different regions of the small intestine, and across the two sexes.

While our prior study provided a framework to study mechanisms of ENS homeostasis, *in vivo* thymidine analogue-based methods allow for quantifying new-born cells but require administration of chemicals over several days, and thus do not permit the study of ongoing neurogenesis at any given time. As a result, a real time assessment of neurogenic niches at different states (steady or perturbed) cannot be performed. Furthermore, the methodologies used for providing evidence of neurogenesis are cumbersome and cannot be translated to human

tissues. Thus, there is a need to simplify the protocols to facilitate better assessment of neurogenesis both in mice and in human specimens.

To address these issues, a simple immunofluorescence-based assay was developed, demonstrating that a subset of adult myenteric neurons immunolabel with antibodies against the established DNA replication and cell proliferation marker phospho-Histone H3 (pH3). Notably, the prevalence of pH3-immunoreactive neurons in healthy tissue matches the rate of neurogenesis previously established by us using thymidine analogues. Additionally, a subset of human adult enteric neurons demonstrate immunoreactivity to both pH3 and the apoptosis marker Cleaved Caspase 3 (CC3). Finally, while the proportions of pH3-immunoreactive neurons were found to be conserved between two different small intestinal regions and across sex, the rate of neuronal birth and neuronal loss varied as a function of ganglia size. New-born neurons were more represented in smaller ganglia than larger ganglia, whereas larger ganglia contained more apoptotic neurons than smaller ganglia. By showing that smaller ganglia are more neurogenic and larger ganglia are more apoptotic, our results suggest that ganglia size is plastic, adding further evidence to the dynamic nature of the adult ENS.

Methods:

Animals: Experimental protocols were approved by The Johns Hopkins University's Animal Care and Use Committee in accordance with the guidelines provided by the National Institutes of Health. Age matched 2 – 3 month old adult wildtype C57BL/6 mice were used.

Tissue preparation: Mice were anesthetized with isoflurane and sacrificed by cervical dislocation. For small intestinal tissue isolation, a laparotomy was performed, and the ileum was removed and lavaged with PBS containing penicillin-streptomycin (Pen-Strep; Invitrogen), then cut into 1-cm-long segments, such that segments from duodenum, jejunum, and ileum were separated. Next,

tissues were placed over a sterile plastic rod and a superficial longitudinal incision was made along the serosal surface and the longitudinal muscle containing myenteric plexus (LM-MP) was peeled off from the underlying tissue using a wet sterile cotton swab[7] and placed in Opti-MEM medium (Invitrogen) containing Pen-Strep. The tissue was then laid flat and fixed with freshly prepared ice cold 4% paraformaldehyde (PFA) solution for 45 minutes in the dark. All LM-MP tissues post-isolation were fixed within 30 minutes of their isolation. After the fixation, the tissue was stored in ice cold sterile PBS with Pen-Strep for immunofluorescence staining and subsequent microscopy.

Immunochemistry: For murine tissue: The fixed LM-MP tissue was washed twice in ice-cold PBS in the dark at 16°C. The tissue was incubated in blocking-permeabilizing buffer (BPB; 5% normal goat serum with 0.3% Triton-X) for 1 hour, followed by incubation with either the combination of of anti-pH3 antibody (Sigma, 1:500) and ANNA-1 (1:1000; patient antisera against the neuronal Hu antigens), or the combination of anti-Cleaved Caspase 3 (Asp175, Cell Signaling, 1:250) and ANNA-1(1:1000) for 48 h at 16°C in the dark with shaking at 55 rpm. The tissues were then washed three times (15-min wash each) in PBS at room temperature in the dark, and incubated in the appropriate secondary antibody (Anti-human 488 and Anti-rabbit 647, Invitrogen, both at 1:500) at room temperature for 1 hour while on a rotary shaker (65 rpm). The tissues were again washed three times in PBS at room temperature, counterstained with DAPI to stain the nuclei, overlaid with Prolong Antifade Gold mounting medium, cover-slipped, and imaged.

For formalin fixed paraffin embedded (FFPE) human tissue: Use of commercially procured human tissue was approved by the Institutional Review Board of the Johns Hopkins University. FFPE tissue sections of human small intestinal tissue were procured through a commercial vendor (Precision for Medicine). To process them, slides were deparaffinized and rehydrated by immersion through the following solutions: 1) Three washes (5 minutes each) with Xylene; 2) two washes with 100% ethanol (10 minutes each); 3) two washes with 95% ethanol (10 minutes each);

4) two washes with 70% ethanol (10 minutes each); 5) two washes with 50% ethanol (10 minutes each); and finally 6) two washes with deionized water (5 minutes each). Next, using pre-heated EDTA buffer (at 90ºC, pH 9.0; 5 mL of 20x EDTA stock solution in 85 ml of deionized water), 30-minute antigen retrieval was performed in a vegetable steamer for humidified conditions. The slides were then cooled in room-temperature PBS. Slides were marked with a hydrophobic pen around the sections, and then blocked and permeabilized in BPB for 1 hour. Buffer was washed off and sections were incubated with either the combination of anti-pH3 antibody (Sigma, 1:250) and ANNA-1 (1:500), or the combination of anti-Cleaved Caspase 3 (1:250) and ANNA-1 (1:500) for 24 h at 16°C in the dark. Following incubation with primary antibody, the sections were washed three times for 15-minutes each in PBS at room temperature in the dark, then incubated with the appropriate secondary antibodies (Invitrogen Anti-human 488 and Anti-rabbit 647; both at 1:500) at room temperature for 1 hour. Next, the sections were again washed three times in PBS at room temperature, counterstained with DAPI to stain the nuclei, overlaid with Prolong Antifade Gold mounting medium, cover-slipped, and imaged.

Microscopy: Microscopy was performed using the oil immersion 40X objective on the Olympus Fluoview 3000rs confocal microscope with galvano and resonance scanning mode, and with 20X magnification of the EVOS M7000 microscope. Control tissues that were immunostained with secondary antibodies only were used to set the threshold laser intensities. All ANNA-1/Hu-immunostained neurons were included in the analysis.

Results:

Adult murine small intestinal myenteric ganglia show evidence of cell proliferation. By using antibodies against the protein phospho-Histone H3 (pH3; phosphorylated at residue Ser10, Sigma), a widely accepted marker for DNA synthesis and cell proliferation[9-13], in conjunction with

ANNA-1 antisera against the pan-neuronal marker Hu, we observed that the adult healthy small intestinal LM-MP tissue contains diverse cell populations of pH3 immunostained cells that are present both within and outside of the myenteric ganglia (Fig 1 a, b). Importantly, the pH3-positive, intra-ganglionic cell population comprises of Hu-immunostained neurons, as well as other unlabeled cells that we assume to be populations of proliferating enteric glial cells[14] and enteric neuronal precursor cells, that we have previously shown to express Nestin and Ki-67[7]. The nuclear presence of the validated and accepted cell proliferation marker pH3 in a population of neurons suggests that these cells have undergone DNA replication and cell proliferation recently, and hence are new-born neurons. Similar to our earlier observations[7], Cleaved Caspase 3 (CC3) immunoreactivity, which indicates apoptotic cells, was found restricted to a subset of myenteric neurons (Fig 1 c).

Human small intestinal myenteric ganglia show evidence of neuronal turnover. We next tested whether the adult human small intestinal myenteric plexus tissue also shows evidence of significant cell proliferation through the presence of pH3-immunoreactive neurons. Using FFPE tissue sections, we found that many cells in the human gut wall also showed immunoreactivity against the DNA replication and cell proliferation marker pH3. Many of these pH3 immunoreactivities were found in nuclei of ganglionic cells, including in the nuclei of Hu-immunolabeled neurons (Fig 2a, b), providing evidence that our observations of pH3 immunoreactivity in adult murine small intestinal myenteric neurons also extend to adult human small intestinal myenteric neurons. Similarly, we also found that the apoptotic marker Cleaved Caspase 3 was detected in a subset of human small intestinal myenteric neurons (Fig 2c). Taken together, these results show that similar to our observations in murine tissue, neuronal birth and neuronal loss, which together drive neuronal turnover, also occur in the healthy human ENS.

Significant proportions of adult small intestinal myenteric neurons show evidence of recent DNA synthesis. Since co-immunolabeling with antibodies against pH3 and pan-neuronal

marker Hu (Fig 1) provides evidence of recent DNA synthesis in adult small intestinal myenteric neurons, we next quantified the proportions of pH3-immunoreactive adult murine small intestinal myenteric neurons in healthy adult mice. By confocal microscopy, we observed 2577 Hu-immunolabeled neurons from the small intestines of 6 adult healthy male and female mice (n = 3 of either sex), which included myenteric plexus tissue from both duodenum and ileum. We found that 8.54% ± 1.09 (mean ± SEM) of all Hu-immunolabeled neurons also showed co-immunolabeling with anti-pH3 antibodies.

Next, we analyzed whether neuronal pH3 immunoreactivity in the ileum or duodenal myenteric ganglia showed any sex bias. In the duodenal myenteric ganglia, we counted 670 neurons in tissues from female mice and 601 neurons in the tissues from male mice (n = 3 of either sex), and found no significant difference between the percentage of pH3-immunoreactive neurons between the two sexes (mean ± SEM $pH3^+$ neurons: female mice = 11.63 ± 2.00; male mice = 6.26 ± 0.75; p = 0.17, Unpaired t-test with Welch's correction, Fig 3a). In the ileal myenteric ganglia, we counted 667 neurons in the tissues from female mice and 639 neurons in the tissues from male mice (n = 3 of either sex), and found no significant difference between the percentage of pH3-immunoreactive neurons between the two sexes (mean ± SEM $pH3^+$ neurons: female mice = 9.93 ± 0.92; male mice = 6.82 ± 0.34; p = 0.06, Unpaired t-test with Welch's correction, Fig 3b). Finally, we compared neuronal pH3 immunoreactivity in ileum vs the duodenal tissue across the two sexes and found no significant difference (Duodenal tissue: neurons counted = 1271, mean ± SEM $pH3^+$ neurons: 8.64 ± 1.52; Ileal tissue: neurons counted = 1306, mean ± SEM pH3+ neurons: 8.38 ± 0.82; p = 0.88, Unpaired t-test with Welch's correction, Fig 3c).

Ganglia size is inversely correlated with proportions of new-born neurons. We have previously shown that there is a significant heterogeneity in ganglia size, where small intestinal myenteric ganglia from healthy mice can contain as little as 3 neurons or contain more than 100 neurons[8]. The myenteric ganglia size in the current study ranged from 3 – 56 neurons (in 145

duodenal and ileal ganglia from male and female mouse) and we next tested whether ganglia size in the adult healthy small intestinal myenteric plexus correlates with the proportions of new-born neurons. We found that the proportion of pH3 immunoreactivity in Hu-expressing neurons in myenteric ganglia decreased significantly with ganglia size ($F = 3.955$; Dfn, DFd = 1, 143; $p = 0.0487$; Simple Linear Regression; Fig 3d).

Ganglia size is directly correlated with proportions of apoptotic neurons. We next tested whether there was any correlation between ganglia size and the proportions of CC3-immunoreactive apoptotic neurons in the adult healthy murine small intestinal myenteric plexus. We quantified the percent of CC3-immunoreactive neurons from 83 myenteric ganglia from 3 mice, where the myenteric ganglia size ranged from 3 – 58 neurons. We found that the proportion of $CC3^+$ Hu-expressing neurons in small intestinal myenteric ganglia increased significantly with ganglia size ($F = 18.25$; Dfn, DFd = 1, 81; $p < 0.0001$; Simple Linear Regression; Fig 3e).

Discussion:

Using multiple lines of evidence we previously showed that significant neurogenesis and neuronal apoptosis occur in the healthy small intestinal myenteric plexus in the adult murine gut[7]. This involved detection of halogenated thymidine analogues, however thymidine analogue-based assays require cumbersome methods to detect evidence of DNA replication and cannot be translated to human tissues or be used for current assessment of ongoing neurogenesis. Herein, we addressed this limitation by using a commonly available tool – validated and established antibodies against a known DNA replication and cell proliferation marker phospho-Histone H3 (pH3)[9-13], along with established antibodies against apoptotic marker Cleaved Caspase 3 – to show the dynamic nature of the myenteric ganglia and the adult enteric nervous system. Taking pH3-immunoreactivity as a surrogate for a new-born cell, we provide evidence that that the adult

healthy murine gut wall contains a significant proportion of new-born neurons, and that the overall proportions of these new-born neurons in the small intestinal tissue remain constant irrespective of sex or location throughout the small intestine. Our prior study demonstrated that almost 90% of adult small intestinal neurons were generated during a 2-week period, and that on any given day ~10% of neurons were newly born[7]. Here, we show that 8 – 10% of adult small intestinal myenteric neurons are immunoreactive for the DNA replication and cell cycle marker pH3, and we infer these to be new-born neurons. This observation closely matches the expected rate of neurogenesis from our previous report[7]. Similarly, as with our earlier report[7], here we again showed the presence of a subpopulation of adult murine small intestinal myenteric neurons that showed detectable presence of the apoptotic marker Cleaved Caspase 3.

This immunohistochemical analyses of new-born and apoptotic neurons in the murine small intestinal myenteric plexus also allowed us to test whether the two processes driving neuronal turnover occur equally in all myenteric ganglia. Our observation that these two processes occur unequally in ganglia of different sizes provide us with a newer understanding of how neuronal turnover occurs in the context of overall ENS structure. Our observations that the smaller ganglia had higher proportions of new-born neurons and larger ganglia had higher proportions of apoptotic neurons suggest that size of myenteric ganglia is plastic. These results would suggest a dynamic model of ENS structure wherein size of myenteric ganglia size wax and wane, as the smaller, more neurogenic ganglia with lower rate of neuronal loss would exhibit more growth and the larger more apoptotic ganglia with lower rate of neuronal birth would shrink and retract in size. In such a scenario, pathological alterations either in neurogenesis or in neuronal loss would skew the proportions of smaller and larger ganglia to cause intestinal dysmotility. Whether such a ganglia size-associated skew in genesis and loss of neurons extends to human tissue is still unknown, however a recent study by Boschetti et al[15] shows that patients with dysmotility have significantly reduced neuronal numbers in myenteric ganglia or have smaller ganglia size. Thus,

these initial observations are significant in our understanding of ENS structure at health and in disease and underscore the need for further and more elegant experiments to better understand the dynamics of ENS structure.

Compared to the arduous and complex protocols required for detection of thymidine analogues such as BrdU in adult enteric neurons[7], our current report provides a simpler method to show the presence of neurogenesis in the adult ENS, and provides a tool that can be used to test alterations in the rate of neurogenesis in response to disease or intervention. In a recent report and subsequent correspondence, Virtanen et al.[16,17] were unable to detect any thymidine analogues in myenteric neurons and suggested that proliferation of glial cells and turnover of neurons in the adult small intestinal ENS are rare events. Although we and others use multiple lines of evidence to show the presence of apoptosis in the adult healthy myenteric neurons of the murine gut[4-7,18-20], Virtanen et al. opined that at least for some of these studies, the observations of a significant rate of apoptosis in myenteric neurons may be due to sampling biases, and that based on their lack of BrdU detection, there is little DNA replication in adult enteric neurons in a healthy gut[16,19]. We understand that faithfully following cumbersome protocols may be a challenge, and hence the simple methodology employed in our current study will provide investigators with an important tool with which they can confidently test ENS tissue for the presence of DNA replication, which is the hallmark of the genesis of new cells.

In this report, by performing immunohistochemistry on human tissue from archived formalin fixed paraffin embedded (FFPE) tissue blocks using the two markers pH3 and CC3 for neurogenesis and neuronal apoptosis, respectively, we detected the presence of new-born and apoptotic neurons in the human small intestinal myenteric ganglia. The detected CC3 immunoreactivity in human myenteric neurons follows other reports of significant proportions of human enteric neurons expressing apoptotic markers in pathologically normal specimens of the human gut[4,5,18]. For example, Chandrasekharan et al. quantified that ~5% of all peripherin-immunoreactive

myenteric neurons in the normal human colonic tissue show immunoreactivity for CC3 and hence are apoptotic neurons[18]. Similarly, Kozlowska et al. showed that a significant proportion of myenteric neurons in the human gastric and colonic myenteric plexus tissues immunolabel with markers of apoptosis[4,5]. Thus, through a simple immunohistochemical technique, we show that the process of neuronal turnover may not be unique to the rodent gut, as new-born and apoptotic neurons are evident in the human gut as well. Previous studies have demonstrated that bacterial components mediate enteric neurogenesis in the murine colon[21], and lipopolysaccharide and flagellin influence HuC/D and pH3-immunoreactive murine enteric neuronal precursors *in vitro*. As such, future studies investigating regulators of ENS plasticity in murine and human small intestine are necessary.

Overall, this study supports the concept of a dynamic ENS in both murine and adult human tissue, with a capacity for both neurogenesis and apoptosis. In addition to facilitating easy quantification of neurogenesis in the murine gut, our report will drive future studies on whether proportions of new-born and apoptotic neurons in the adult human gut show a similar unequal distribution across ganglia of various sizes. This report also provides investigators with an established protocol to study how the rate of neurogenesis in the adult human gut may change throughout life and in different disease conditions of intestinal dysmotility.

Acknowledgements: SK was supported by an R01 grant from the National Institute of Aging (R01AG66768) and a pilot award from the Diacomp foundation. AG was supported by a Fulbright Future Scholarship, funded by The Kinghorn Foundation.

Figures

Figure 1: DNA proliferation marker phospho-histone H3 (pH3) is detected in neurons and other cells of the adult healthy myenteric plexus tissue. (a) Longitudinal muscle and myenteric plexus tissue (LM-MP) from an adult healthy mouse, when stained with antibodies against phospho-Histone H3 (pH3, green) and the pan-neuronal marker Hu (red) shows the presence of pH3 immunoreactivity in ganglionic cells that do express Hu (yellow arrow) and those that don't express Hu (cyan arrow). pH3 immunoreactivity is also detected in extra-ganglionic cells in this tissue (white arrow) that are presumed to be longitudinal muscle cells. (b) Magnified image of a myenteric ganglia labeled with antibodies against pH3 (green) and Hu (red) again show the presence of pH3-immunoreactive Hu-immunolabeled new-born neurons (yellow arrow), along with neurons that are not immunoreactive against Hu (white arrow) and pH3-immunoreactive extra-ganglionic cells (cyan arrow). (c) Representative image of the adult murine small intestinal LM-MP tissue, when stained with antibodies against Cleaved Caspase 3 (CC3, red) and the pan-neuronal marker Hu (green), shows the presence of CC3 immunoreactivity in a subset of Hu-immunoreactive neurons (yellow arrows), while other neurons in the same and other ganglia do not immunolabel for CC3 (green arrow). Nuclei are labeled with DAPI (blue), and scale bar indicates 10 µm.

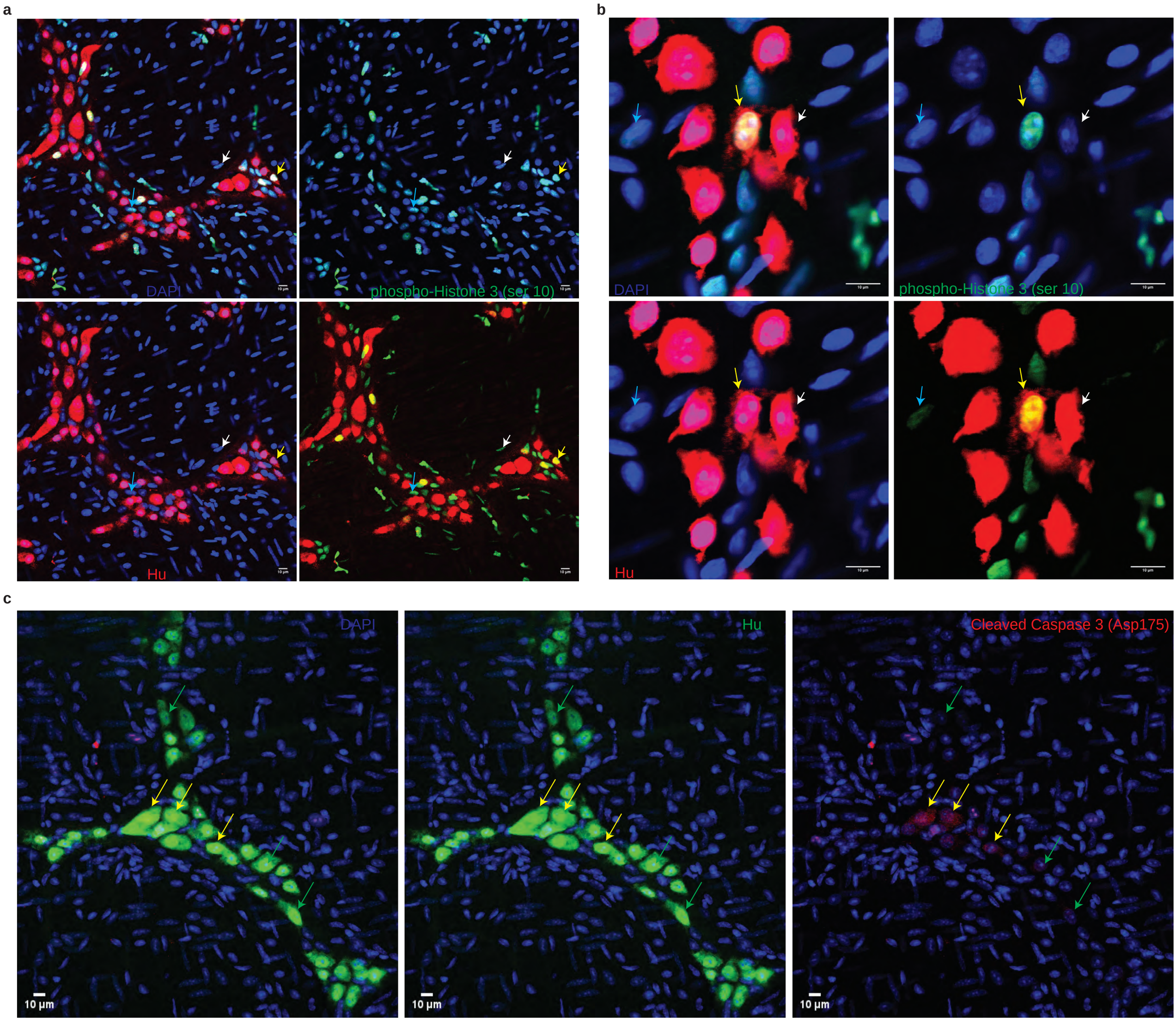
a
DAPI
phospho-Histone 3 (ser 10)
Hu
b
DAPI
phospho-Histone 3 (ser 10)
Hu
c
DAPI
Hu
Cleaved Caspase 3 (Asp175)
10 µm
10 µm
10 µm

Figure 1

Figure 2: New-born and apoptotic neurons are observed in human small intestinal myenteric ganglia. (a) Formalin fixed paraffin embedded (FFPE) tissue sections from adult human small intestine with immunolabelling of pH3 (red) and Hu (green) show the presence of pH3-immunoreactive neurons. (b) Magnified inset from (a). (c) Orthogonal views of a myenteric ganglia immunostained with antibodies against CC3 (red) and Hu (green) show the presence of CC3-immunolabeled neurons. (d) Representative image of a myenteric ganglia immunostained with antibodies against Hu (green) but no primary antibodies for the red channel shows a lack of non-specific staining with the secondary antibodies. Nuclei are labeled with DAPI (blue) and scale bar indicates 10 µm.

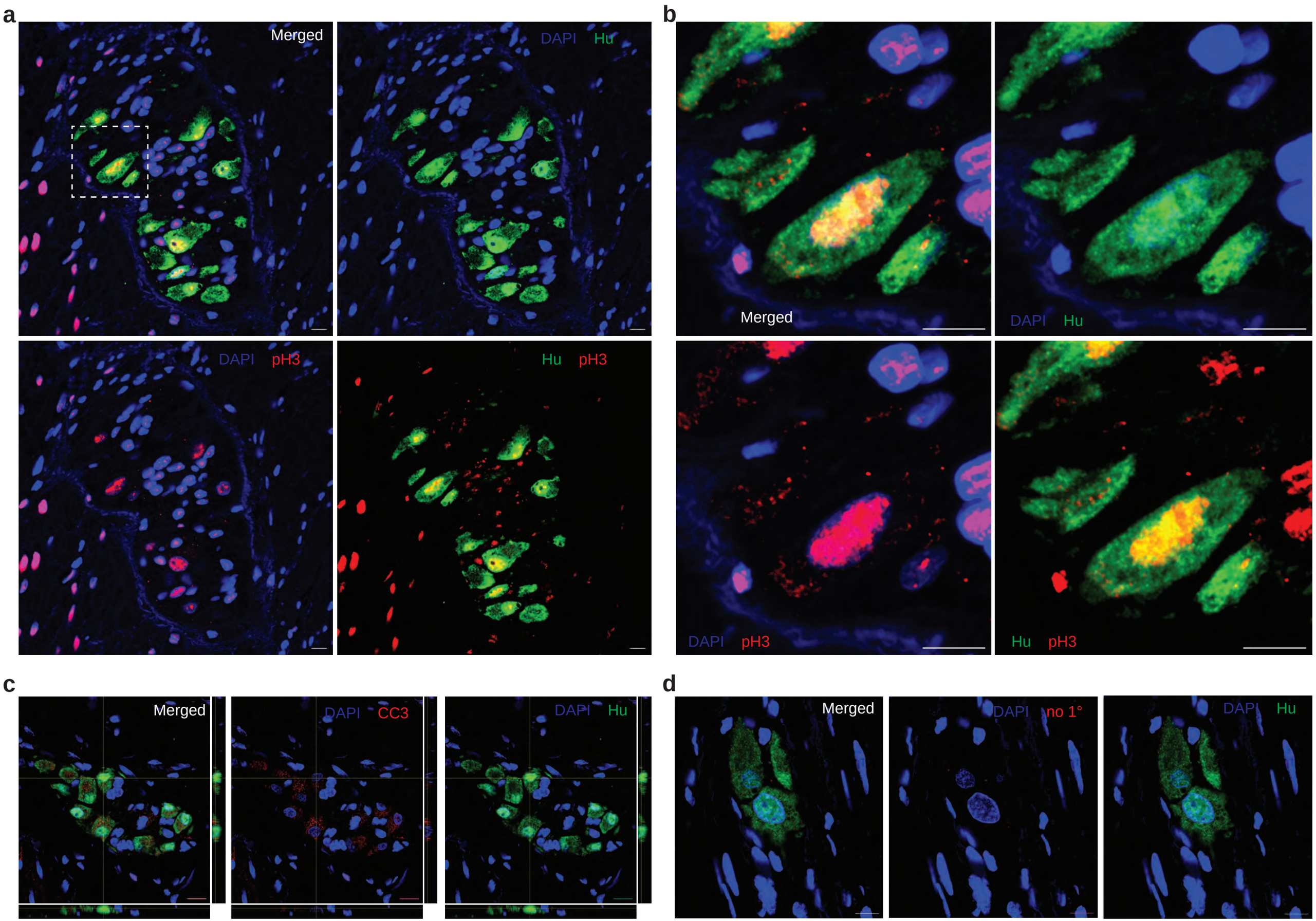
a
Merged
DAPI Hu
DAPI pH3
Hu pH3
b
Merged
DAPI Hu
DAPI pH3
Hu pH3
c
Merged
DAPI CC3
DAPI Hu
d
Merged
DAPI no 1°
DAPI Hu

Figure 2

Figure 3: Quantifications of pH3- and CC3-immunoreactive neurons in the adult murine gut. (a) Quantification of pH3-immunoreactive neurons in the duodenal tissue of age-matched male and female mice show no significant sex-bias in their proportions ($p > 0.05$, Students' t-test). (b) Quantification of pH3-immunoreactive neurons in the ileal tissue of age-matched male and female mice show no significant sex-bias in their proportions ($p > 0.05$, Students' t-test). (c) Quantification of pH3-immunoreactive neurons in the duodenal and ileal tissue of age-matched mice show no significant differences in their proportions between the two tissue regions ($p > 0.05$, Students' t-test). (d) Simple linear regression analyses of prevalence of pH3-immunoreactive neurons in small intestinal ganglia containing various numbers of neurons shows a significant inverse correlation between pH3-immunoreactivity and the ganglia size, where smaller ganglia have significantly higher prevalence of pH3-immunoreactive neurons than larger ganglia. The equation defines the slope of the curve ($R^2 = 0.0269$). Regression line is depicted in black and error bars are depicted in gray. (e) Simple linear regression analyses of prevalence of CC3-immunoreactive neurons in small intestinal ganglia containing various numbers of neurons shows a significant direct correlation between CC3-immunoreactivity and the ganglia size, where smaller ganglia have significantly lower prevalence of CC3-immunoreactive neurons than larger ganglia. The equation defines the slope of the curve ($R^2 = 0.1839$). Regression line is depicted in black and error bars are depicted in gray.

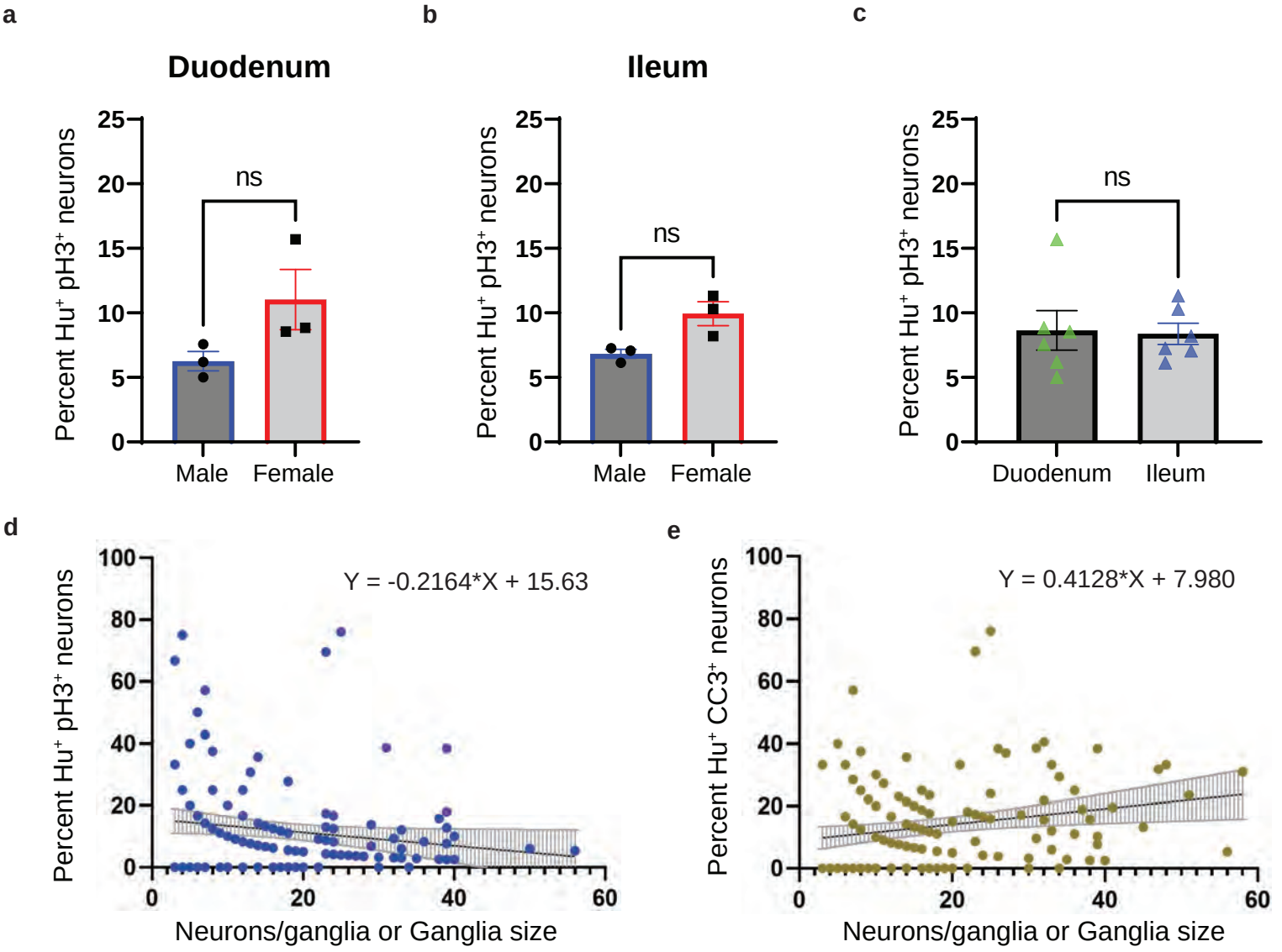
a
Duodenum
Percent Hu+ pH3+ neurons
25
20
15
10
5
0
ns
Male
Female
b
Ileum
Percent Hu+ pH3+ neurons
25
20
15
10
5
0
ns
Male
Female
c
Percent Hu+ pH3+ neurons
25
20
15
10
5
0
ns
Duodenum
Ileum
d
Percent Hu+ pH3+ neurons
100
80
60
40
20
0
Y = -0.2164*X + 15.63
0
20
40
60
Neurons/ganglia or Ganglia size
e
Percent Hu+ CC3+ neurons
100
80
60
40
20
0
Y = 0.4128*X + 7.980
0
20
40
60
Neurons/ganglia or Ganglia size

Figure 3

References

1 Gregersen, H. & Kassab, G. Biomechanics of the gastrointestinal tract. *Neurogastroenterology and motility : the official journal of the European Gastrointestinal Motility Society* **8**, 277-297, doi:10.1111/j.1365-2982.1996.tb00267.x (1996).

2 Sherman, M. P., Zaghouani, H. & Niklas, V. Gut microbiota, the immune system, and diet influence the neonatal gut-brain axis. *Pediatr Res* **77**, 127-135, doi:10.1038/pr.2014.161 (2015).

3 Hyland, N. P. & Cryan, J. F. Microbe-host interactions: Influence of the gut microbiota on the enteric nervous system. *Dev Biol* **417**, 182-187, doi:10.1016/j.ydbio.2016.06.027 (2016).

4 Kozlowska, A., Kozera, P., Majewski, M. & Godlewski, J. Co-expression of caspase-3 or caspase-8 with galanin in the human stomach section affected by carcinoma. *Apoptosis* **23**, 484-491, doi:10.1007/s10495-018-1470-y (2018).

5 Kozlowska, A. *et al.* Myenteric plexuses atrophy in the vicinity of colorectal cancer tissue is not caused by apoptosis or necrosis. *Folia Histochem Cytobiol* **54**, 99-107, doi:10.5603/FHC.a2016.0012 (2016).

6 Nezami, B. G. *et al.* MicroRNA 375 mediates palmitate-induced enteric neuronal damage and high-fat diet-induced delayed intestinal transit in mice. *Gastroenterology* **146**, 473-483 e473, doi:10.1053/j.gastro.2013.10.053 (2014).

7 Kulkarni, S. *et al.* Adult enteric nervous system in health is maintained by a dynamic balance between neuronal apoptosis and neurogenesis. *Proceedings of the National Academy of Sciences*, 201619406 (2017).

8 Kobayashi, Y. *et al.* COUNTEN, an AI-Driven Tool for Rapid and Objective Structural Analyses of the Enteric Nervous System. *eneuro* **8**, ENEURO.0092-0021.2021, doi:10.1523/eneuro.0092-21.2021 (2021).

9 An, Z. *et al.* A quiescent cell population replenishes mesenchymal stem cells to drive accelerated growth in mouse incisors. *Nat Commun* **9**, 378, doi:10.1038/s41467-017-02785-6 (2018).

10 Alonso-Martin, S. *et al.* SOXF factors regulate murine satellite cell self-renewal and function through inhibition of beta-catenin activity. *Elife* **7**, doi:10.7554/eLife.26039 (2018).

11 Tiede, S. *et al.* The FAK inhibitor BI 853520 exerts anti-tumor effects in breast cancer. *Oncogenesis* **7**, 73, doi:10.1038/s41389-018-0083-1 (2018).

12 Rotelli, M. D. *et al.* A Cyclin A-Myb-MuvB-Aurora B network regulates the choice between mitotic cycles and polyploid endoreplication cycles. *PLoS Genet* **15**, e1008253, doi:10.1371/journal.pgen.1008253 (2019).

13 Jiang, Y. H. *et al.* Re-enforcing hypoxia-induced polyploid cardiomyocytes enter cytokinesis through activation of beta-catenin. *Sci Rep* **9**, 17865, doi:10.1038/s41598-019-54334-4 (2019).

14 Zeisel, A. *et al.* Molecular Architecture of the Mouse Nervous System. *Cell* **174**, 999-1014 e1022, doi:10.1016/j.cell.2018.06.021 (2018).

15 Boschetti, E. *et al.* Enteric neuron density correlates with clinical features of severe gut dysmotility. *Am J Physiol Gastrointest Liver Physiol* **317**, G793-G801, doi:10.1152/ajpgi.00199.2019 (2019).

16 Virtanen, H., Garton, D. & Andressoo, J.-O. Reply. *Cellular and Molecular Gastroenterology and Hepatology* **14**, 968-969, doi:10.1016/j.jcmgh.2022.07.004 (2022).

17 Virtanen, H., Garton, D. R. & Andressoo, J.-O. Myenteric Neurons Do Not Replicate in Small Intestine Under Normal Physiological Conditions in Adult Mouse. *Cellular and Molecular Gastroenterology and Hepatology* **14**, 27-34, doi:10.1016/j.jcmgh.2022.04.001 (2022).

18 Chandrasekharan, B. *et al.* Colonic motor dysfunction in human diabetes is associated with enteric neuronal loss and increased oxidative stress. *Neurogastroenterology & Motility* **23**, 131-e126, doi:https://doi.org/10.1111/j.1365-2982.2010.01611.x (2011).

19 De Schepper, S. *et al.* Self-Maintaining Gut Macrophages Are Essential for Intestinal Homeostasis. *Cell* **175**, 400-415 e413, doi:10.1016/j.cell.2018.07.048 (2018).

20 Becker, L. *et al.* Age-dependent shift in macrophage polarisation causes inflammation-mediated degeneration of enteric nervous system. *Gut*, gutjnl-2016-312940 (2017).

21 Yarandi, S. S. *et al.* Intestinal Bacteria Maintain Adult Enteric Nervous System and Nitrergic Neurons via Toll-like Receptor 2-induced Neurogenesis in Mice. *Gastroenterology* (2020).